Multifield, temperature and concentration dependence of spin relaxation and local motion in 2,2-propane diyl-bis(4-hydroxyphenyl) polyformal

Chi-Cheng Hung, John H. Shibata and Alan Anthony Jones*
Jeppson Laboratory, Department of Chemistry, Clark University, Worcester, MA 01610 USA

and Paul T. Inglefield
Department of Chemistry, College of the Holy Cross, Worcester, MA 01610, USA
(Received 9 June 1986; revised 22 August 1986; accepted 2 October 1986)

^{13}C and proton spin-lattice relaxation data were determined as a function of field, temperature and concentration for 2,2-propane diyl-bis(4-hydroxyphenyl) polyformal in $C_2D_2Cl_4$. The concentration of polymer was varied from a few per cent by weight up to the bulk rubber and temperature was varied from $-20°C$ to $+120°C$. The relaxation data is interpreted in terms of several local motions including segmental motion, phenylene group rotation, methyl group rotation and formal group rotation. Segmental motion is described by a correlation function developed by Hall and Helfand which allows for cooperative and single bond transitions. The phenylene group rotation is described by the Woessner anisotropic stochastic diffusion model except at high concentration (≥ 50 wt %) where the phenylene data is simulated by restricted rotation. Methyl group rotation is described by the Woessner three fold jump model, and the formal group rotation is described by double *trans–gauche* rotations about the C–O axes. At a concentration of 5 wt %, the time scale of segmental motion is slightly slower than in bisphenol-A–polycarbonate. However, the time scales of phenylene group and methyl group rotations are nearly identical for both polymers. A comparison is also made with chloral polyformal, another similar polyformal. The effect of concentration on local motion was monitored by ^{13}C spin-lattice relaxation measurements at three Larmor frequencies over the range of 5 to 100 wt % polymer at a temperature 40°C above the glass transition of this polyformal. The rate of local chain motion decreases as the concentration of polymer increases with the exception of methyl group rotation which remains constant. The correlation times for several local backbone motions are fit to free volume theory which yields a fractional free volume of 0.38 for the solvent ($C_2D_2Cl_4$) and 0.28 for the polymer.

(Keywords: spin relaxation; local motion; dissolved polymer)

INTRODUCTION

Spin relaxation in dilute solution has been widely studied in the last decade[1]. One of these efforts has focused on characterizing local chain motions in polymers with rather complex repeat units such as the polycarbonates. The early dilute solution studies focused on bisphenol-A–polycarbonate (BPA–PC) and its structural analogues[2–6]. Polyformal is such a structural analogue with the carbonate replaced by the formal link. The formal link presents an opportunity to monitor chain dynamics at an additional site and the added information allows for a more complete characterization of local motions. A polyformal, Chloral–PF, shown in *Figure 1*, has already been studied in the dilute solution by ^{13}C, proton and deuterium n.m.r.[7,8] The polymer of interest in this report, 2,2-propane diyl-bis(4-hydroxyphenyl) polyformal, abbreviated BPA–PF, is similar in structure to Chloral–PF. Therefore, a very similar dynamical description is applied and a comparison of chain dynamics between the two polyformals may be made. Also the motional model[8] developed for Chloral–PF is quite detailed and can be further tested by the large data base in this study of a closely related system.

In addition to a dilute solution study, the lower T_g of BPA–PF (90°C) makes possible an examination of local chain dynamics from dilute solution through concentrated solutions to the rubber state. The concentration dependence of the local motion was monitored by ^{13}C T_1 measurements at three Larmor frequencies at a temperature above T_g. In general, much less attention is paid to local motion in polymers in concentrated solutions, melts and rubbers. A few interesting and significant spin-lattice relaxation studies have been carried out[9–13] but the number of reports and depth of interpretation is limited relative to the dilute solution and glass states. Although the measurement of T_1 as a function of Larmor frequency is probably the best approach to characterize the short-range chain motion in concentrated solutions and rubbers, this approach has not been widely used. The standard T_1 measurements of ^{13}C and deuterium relaxation[13] at high concentrations are straightforward with only some minor problems due to signal overlap. Isotopic labelling can also be employed to avoid signal overlap problems on specifically labelled systems in deuterium n.m.r. experiments[13] but frequently

0032-3861/87/071062-09$03.00

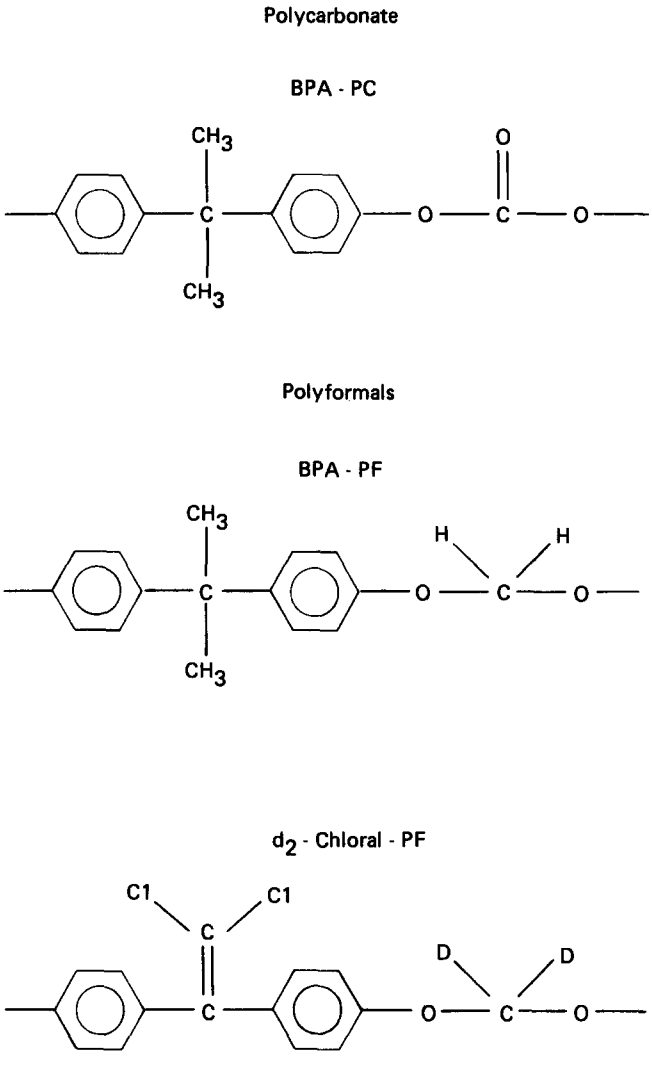

Figure 1 Structure of the repeat units and the associated abbreviations

high resolution ^{13}C spectra without overlap can be obtained with low power scalar decoupling[14] if measurements are made somewhat above the glass transition[9].

EXPERIMENTAL

High molecular weight samples of BPA–PF were kindly supplied by General Electric. A 5 wt% solution in $C_2D_2Cl_4$ was prepared for proton and ^{13}C spin relaxation measurements while 10, 30, 50, 70 and 100 wt% were prepared for ^{13}C spin relaxation measurements. These samples were subjected to five freeze–pump–thaw cycles before sealing.

The 90 MHz proton measurement, and the 22.6 MHz ^{13}C measurement were obtained on a Bruker SXP 20-100 spectrometer. The 250 MHz proton, 62.9 MHz ^{13}C measurement were obtained on a Bruker WM-250 spectrometer. The 125 MHz ^{13}C measurement was obtained on a Bruker WM-500 at Yale University. All T_1 measurements were made with a standard 180°–τ–90° sequence and a temperature calibration was performed on each instrument. For the SXP, a thermocouple was inserted into the probe, while for the WM-500 and WM-250, the chemical shift vs. temperature method was employed. The standard calibration samples were ethylene glycol for high temperature and methanol for low temperature. The experimental error in the reported T_1 values is 10%, which included errors in sample preparation, temperature control, pulse widths and data fitting.

RESULTS

The recovery of magnetization to equilibrium monitored in the 180°–τ–90° sequence follows a simple exponential dependence on delay time τ. The data are fit using a standard linear least-squares algorithm and a nonlinear least-squares algorithm. Both analyses yield T_1 values within 10% of each other and average values are reported. No evidence of cross-relaxation or cross-correlation is observed in the decay curve of the recovery of magnetization. *Table 1* contains proton and ^{13}C T_1's in the 5 wt% sample as a function of temperature and Larmor frequency. *Table 2* contains ^{13}C T_1's as a function of concentration and Larmor frequency at 130°C.

Interpretation

The standard relationship between T_1's and spectral densities, J, are employed. For ^{13}C the expressions are[3]

$$1/T_1 = W_0 + 2W_{1C} + W_2$$

$$W_0 = \sum_j \gamma_C^2 \gamma_H^2 \hbar^2 J_1(\omega_0)/20 r_j^6$$

$$W_{1C} = \sum_j 3\gamma_C^2 \gamma_H^2 \hbar^2 J_1(\omega_C)/40 r_j^6 \qquad (1a)$$

$$W_2 = \sum_j 3\gamma_C^2 \gamma_H^2 \hbar^2 J_2(\omega_2)/10 r_j^6$$

$$\omega_0 = \omega_H - \omega_C \qquad \omega_2 = \omega_H + \omega_C$$

and for protons the relationship is

$$1/T_1 = \sum_j (9/8)\gamma^4 \hbar^2 r_j^{-6}[(2/15)J_1(\omega_H) + (8/15)J_2(2\omega_H)] \qquad (1b)$$

The internuclear distances employed are 1.09 Å for the phenylene C–H distance, 1.12 Å for the methyl C–H distance, 1.77 Å for the methyl proton–proton distance, 1.135 Å for the formal C–H distance and 1.79 Å for the formal proton–proton distance[4,7].

The expression for the spectral densities can be derived from the action of four local motions on intramolecular internuclear interactions. The motions are segmental rearrangement, phenylene group rotation, methyl group rotation and formal group rotation. The geometry of the various internuclear interactions relative to the four motions allows separate characterization of each of the motions as described before[2,4].

The description of segmental motion employed in the analysis of the data is the Hall–Helfand model[16,17] based on computer simulation of chain dynamics. This description is applied to the flexible backbone bonds of the bisphenol A unit which are shown in *Figure 2*. The correlation function for segmental motion is given by

$$\Phi(t) = \exp(-t/\tau_0)\exp(-t/\tau_1)I_0(t/\tau_1) \qquad (2)$$

where τ_1 is the correlation time for cooperative

Table 1 Spin-lattice relaxation times of BPA–PF in 5 wt% solution[a]

Temperature (°C)	Methyl protons		Methyl carbons		Protonated[b] phenylene carbons	
	250 MHz	90 MHz	62.9 MHz	22.6 MHz	62.9 MHz	22.6 MHz
−20	142	42	51	29	146	83
0	123	60	73	59	181	127
20	134	85	108	96	258	242
40	171	121	158	152	430	393
60	226	166	271	231	703	638
80	311	270	338	330	971	953
100	414	325	545	500	1470	1473
120	554	448	822	730	2451	2158
Temperature (°C)	Formal protons		Formal carbon			
	250 MHz	90 MHz	62.9 MHz	22.6 MHz		
−20	333	100	70	28		
0	268	91	78	49		
20	248	118	104	85		
40	290	162	147	134		
60	359	233	245	195		
80	490	387	315	302		
100	668	554	535	456		
120	935	705	723	685		

[a] All relaxation times in ms
[b] The difference of T_1 from each of the two types of protonated phenylene carbons is within 5% so the average value is reported

Table 2 Spin-lattice relaxation times of BPA–PF at various concentrations[a] and at 130°C

Phenylene carbon			
Wt%	125.7 MHz	62.9 MHz	22.6 MHz
10	2357	2428	1956
30	1423	1366	1123
50	1204	943	606
70	550	475	280
100	396	238	108
Formal carbon			
Wt%	125.7 MHz	62.9 MHz	22.6 MHz
10	933	985	845
30	673	584	462
50	426	361	253
70	258	197	141
100	177	117	64
Methyl carbon			
Wt%	125.7 MHz	62.9 MHz	22.6 MHz
10	802	783	651
30	616	564	473
50	503	469	338
70	393	365	230
100	394	349	212

[a] All relaxation times in ms

conformational transitions involving several bonds, τ_0 is the correlation time for single-bond conformational transitions, and I_0 is a modified Bessel function of order zero. Segmental motion about these bonds, depicted in *Figure 2*, affects the dynamics of phenylene, methyl and formal groups. However, segmental motion produced by repeated independent rotation of the bonds indicated in *Figure 2* leads to complete loss of orientational memory while additional restricted anisotropic rotations of the phenylene methyl and formal groups to be considered

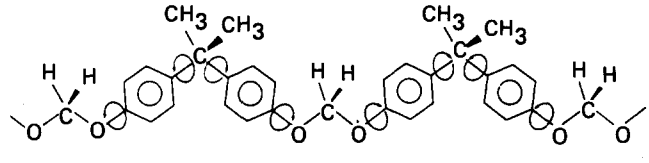

Figure 2 Physical picture of segmental motion within the bisphenol unit. The arrow indicates those bonds in the bisphenol unit whose reorientation is included in the description of segmental motion. Note that repeated independent rotation of the indicated bonds can lead to isotropic segmental motion

later only leads to partial loss of orientational memory of a particular functional group. The correlation function can be Fourier transformed to yield the following spectral density required for calculation of spin relaxation.

$$J(\omega)=2\{[(\tau_0^{-1})(\tau_0^{-1}+2\tau_1^{-1})-\omega^2]^2 + [2(\tau_0^{-1}+\tau_1^{-1})\omega]^2\}^{-1/4} \times \cos\{1/2 \arctan 2(\tau_0^{-1}+\tau_1^{-1})\omega/[(\tau_0^{-1}+2\tau_1^{-1})-\omega^2]\} \quad (3)$$

Local formal, phenylene and methyl group rotations can be described by limited anisotropic internal rotation[18]. In the formal group the appropriate correlation function for a *trans–gauche* two site jump is[8]

$$g_{00}(t)=1$$
$$g_{\pm1\pm1}(t)=g_{\pm2\pm2}(t)=1/4+3/4\exp(-t/\tau_{iff}) \quad (4)$$

where τ_{iff} is the correlation time for the jump. This formal group motion is actually a form of segmental motion though a limited anisotropic internal rotation description can be utilized since a conformational energy calculation

indicates the simple two site jump picture[40]. This description of formal group motion was developed to interpret ^{13}C, proton and deuterium spin lattice relaxation in a closely related polyformal[8].

When the segmental correlation function leads to isotropic motion and the internal correlation function is independent of the initial states, the Szabo formalism[19] can be employed to express the internal correlation function for double rotations about the two C–O bonds of the formal group as[8]

$$G(t)=\sum_{m,p}[d^2_{mo}(\Delta)]^2[d^2_{pm}(\beta_{21})]^2 \; g^{(1)}_{mm}(t)g^{(2)}_{pp}(t) \tag{5}$$

where $d^2_{mo}(\Delta)$ and $d^2_{pm}(\beta_{21})$ are reduced Wigner rotation matrices. Using this formalism, several types of anisotropic motion can be introduced including jumps between three minima or stochastic diffusion.

In the case of one internal rotation axis, the correlation function in equation (5) reduces to,

$$G(t)=\sum_{m}[d^2_{mo}(\Delta)]^2 g_m(t) \tag{6}$$

where $g_m(t)$ is the correlation function developed by Woessner[18]. For stochastic diffusion of phenylene group rotation about the C_1C_4 axis, the correlation function is[4]

$$\begin{aligned} G(t)&=A+B\exp(-t/\tau_{irp})+C\exp(-4t/\tau_{irp})\\ A&=(3\cos^2\Delta-1)^2/4\\ B&=3(\sin^2 2\Delta)/4\\ C&=3(\sin^4\Delta)/4 \end{aligned} \tag{7}$$

where τ_{irp} is the correlation time for phenylene group rotation. For the threefold jump of methyl group rotation, the correlation function is[4]

$$G(t)=A+B\exp(-t/\tau_{irm})+C\exp(-t/\tau_{irm}) \tag{8}$$

where τ_{irm} is the correlation time for methyl group rotation. A, B and C are the same expressions as in equation (7).

The correlation function for segmental motion can be combined with formal group rotation, phenylene group rotation or methyl group rotation to yield a composite correlation function appropriate for a given site in the repeat unit. These composite correlation functions can be Fourier transformed using the general formula,

$$J(\omega)=2\,Re\int_0^\infty \Phi(t)\,G(t)\exp(i\omega t)\,dt \tag{9}$$

By inserting the internal correlation function for formal group motion described by equation (5), and integrating, the spectral density for formal group motion becomes

$$\begin{aligned} J(\omega)=&J_a(\tau_0,\tau_1,\omega)[d^2_{00}(\Delta)]^2[d^2_{00}(\beta_{21})]^2\\ &+(\tfrac{1}{16}J_a(\tau_0,\tau_1,\omega)+\tfrac{3}{8}J_b(\tau_{b0},\tau_1,\omega)+\tfrac{9}{16}J_c(\tau_{c0},\tau_1,\omega))\\ &\times\{2[d^2_{20}(\Delta)]^2([d^2_{22}(\beta_{21})]^2)+[d^2_{2-2}(\beta_{21})]^2\\ &+2[d^2_{10}(\Delta)]^2([d^2_{11}(\beta_{21})]^2\\ &+[d^2_{1-1}(\beta_{21})]^2)+2([d^2_{10}(\Delta)]^2\\ &+[d^2_{20}(\Delta)]^2)([d^2_{21}(\beta_{21})]^2+[d^2_{2-1}(\beta_{21})]^2)\}\\ &+(\tfrac{1}{4}J_a(\tau_0,\tau_1,\omega)+\tfrac{3}{4}J_b(\tau_{b0},\tau,\omega))\times(2([d^2_{00}(\Delta)]^2\\ &+[d^2_{20}(\Delta)]^2)[d^2_{20}(\beta_{21})]^2+2([d^2_{00}(\Delta)]^2\\ &+[d^2_{10}(\Delta)]^2)[d^2_{10}(\beta_{21})]^2) \end{aligned} \tag{10}$$

$$\tau_{b0}^{-1}=\tau_0^{-1}+\tau_{irf}^{-1}$$

$$\tau_{c0}^{-1}=\tau_0^{-1}+(\tau_{irf}/2)^{-1}$$

where $J_a(\tau_0,\tau_1,\omega)$, $J_b(\tau_{b0},\tau_1,\omega)$ and $J_c(\tau_{c0},\tau_1,\omega)$ have the same forms as equation (3) with τ_0 replaced by τ_0, τ_{b0} and τ_{c0}, respectively.

For phenylene group and methyl group rotations, substituting either equations (7) or (8) into equation (9) and integrating, the spectral density becomes

$$J(\omega)=AJ_x(\tau_0,\tau_1,\omega)+BJ_y(\tau_{y0},\tau_1,\omega)+CJ_z(\tau_{z0},\tau_1,\omega) \tag{11}$$

For stochastic diffusion,

$$\tau_{y0}^{-1}=\tau_0^{-1}+\tau_{irp}^{-1}$$

$$\tau_{z0}^{-1}=\tau_0^{-1}+(\tau_{irp}/4)^{-1}$$

For a threefold jump,

$$\tau_{y0}^{-1}=\tau_{z0}^{-1}=\tau_0^{-1}+\tau_{irm}^{-1}$$

The form of J_x, J_y and J_z is the same as in equation (3) with τ_0 replaced by τ_0, τ_{y0} and τ_{z0}, respectively.

Since the formal group, phenylene group and methyl group are either in the backbone or attached to it, we require that the same τ_0 and τ_1 parameters for segmental motion apply to all sites. To simulate the 5 wt% solution data, three parameters (τ_0, τ_1 and τ_{irm}) are determined from four frequencies of methyl carbon and proton data using equation (11). After the segmental description is determined by the selection of τ_0 and τ_1, τ_{irp} can be determined from two frequencies of phenylene carbon data using equation (11) and τ_{irf} can be determined from four frequencies of formal carbon and proton data using equation (10). Note that the two frequencies of phenylene carbon data and the four frequencies of formal data also depend on τ_0 and τ_1 and serve to check the description of segmental motion though each functional group also has an additional degree of motional freedom described by an additional correlation time. Few problems were encountered in the simulation, and essentially all the observed values could be reproduced by simulation within the experimental uncertainty of 10%. *Table 3* contains the simulation parameters. One can calculate apparent activation energies by assuming Arrhenius behaviour and these are included in *Table 3*.

In the concentration study, the interpretation follows the same approach as for the 5 wt% dilute solution except phenylene group motion changes at the higher

Table 3 Simulation results for a 5 wt% solution of BPA–PF in $C_2D_2Cl_4$

Temperature (°C)	τ_1 (ns)	τ_0 (ns)	τ_{irp} (ns)	τ_{irm} (ns)	τ_{irf} (ns)
−20	3.68	7.90	1.53	0.79	3.00
0	1.95	5.00	0.78	0.34	1.52
20	0.84	2.78	0.48	0.20	0.71
40	0.46	1.71	0.26	0.12	0.50
60	0.29	1.15	0.148	0.0695	0.30
80	0.18	0.79	0.097	0.040	0.18
100	0.118	0.57	0.066	0.024	0.10
120	0.085	0.48	0.040	0.013	0.06
E_a (kJ mol^{-1})	22.7	18.1	21.4	23.2	23.4
$\tau_\infty \times 10^{14}$ (s)	7.97	163	6.59	1.32	4.79
Correlation coefficient	0.99	0.99	0.99	0.99	0.99

concentration. The best model for phenylene group rotation from 50 wt% to 100 wt% is a model for restricted rotation about the C_1C_4 axis in addition to segmental motion. A restricted rotation model developed by Gronski[20] has been combined with the Hall–Helfand segmental motion correlation function previously and the composite spectral density can be written as[7]

$$J_i(\omega_i)=AJ_i^{01}(\omega_i)+\frac{B}{l^2}\left\{[(1-\cos l)^2+\sin^2 l]J_i^{01}(\omega_i)\right.$$
$$+\tfrac{1}{2}\sum_{n=1}^{\infty}\left[\left\{\frac{[1-\cos(l-n\pi)]}{(1-n\pi/l)}+\frac{[1-\cos(l+n\pi)]}{(1+n\pi/l)}\right\}^2\right.$$
$$\left.\left.+\left\{\frac{\sin(l-n\pi)}{(1-n\pi/l)}+\frac{\sin(l+n\pi)}{(1+n\pi/l)}\right\}^2\right]J_i^{\lambda_n}(\omega_i)\right\}$$
$$+\frac{C}{2l^2}\left\{\tfrac{1}{2}[(1-\cos 2l)^2+\sin^2 2l]J_i^{01}(\omega_i)\right.$$
$$+\sum_{n=1}^{\infty}\left[\left\{\frac{[1-\cos(2l-n\pi)]}{(2-n\pi/l)}+\frac{[1-\cos(2l+n\pi)]}{(2+n\pi/l)}\right\}^2\right.$$
$$\left.\left.+\left\{\frac{\sin(2l-n\pi)}{(2-n\pi/l)}+\frac{\sin(2l+n\pi)}{(2+n\pi/l)}\right\}^2\right]J_i^{\lambda_n}(\omega_i)\right\}$$

where

$$J_i^{01}(\omega_i)=\{[\tau_0^{-1}(\tau_{01}^{-1}+\tau_1^{-1})-\omega_i^2]^2+(2\tau_{01}^{-1}\omega_i)^2\}^{-1/4}$$
$$\times\cos\left[\tfrac{1}{2}\arctan\frac{2\tau_{01}^{-1}\omega_i}{\tau_0^{-1}(\tau_{01}^{-1}+\tau_1^{-1})-\omega_i^2}\right]$$

and

$$J_i^{\lambda_n}(\omega_i)=\{[\tau_0^{-1}(\tau_{01}^{-1}+\lambda_n)(\tau_{01}^{-1}+\tau_1^{-1}+\lambda_n) \quad (12)$$
$$-\omega_i^2]^2\}^{1/4}\cos\left[\tfrac{1}{2}\arctan\frac{2(\tau_{01}^{-1}+\lambda_n)\omega_i}{(\tau_0^{-1}+\lambda_n)(\tau_{01}^{-1}+\lambda_n)-\omega_i^2}\right]$$

$$\tau_{01}^{-1}=\tau_0^{-1}+\tau_1^{-1}$$

$$\lambda_n=(n\pi/l)^2D_{ir}$$

where $J_i(\omega_i)$ can be substituted into equation (1a) to calculate T_1. D_{ir} is the diffusion constant of the restricted diffusion and l is the angular amplitude of the restricted diffusion. *Table 4* shows the simulation results for each concentration.

The change in correlation time for segmental motion and formal group rotation with concentration can be analysed in terms of free volume theory. According to Kramers theory[21,22], for passage from a well with a parabolic minimum over a barrier with a parabolic top, the probability, P, per unit time is

$$P=(\omega_A\omega_C/2\pi\beta)\exp(-U_0/kT) \quad (13)$$

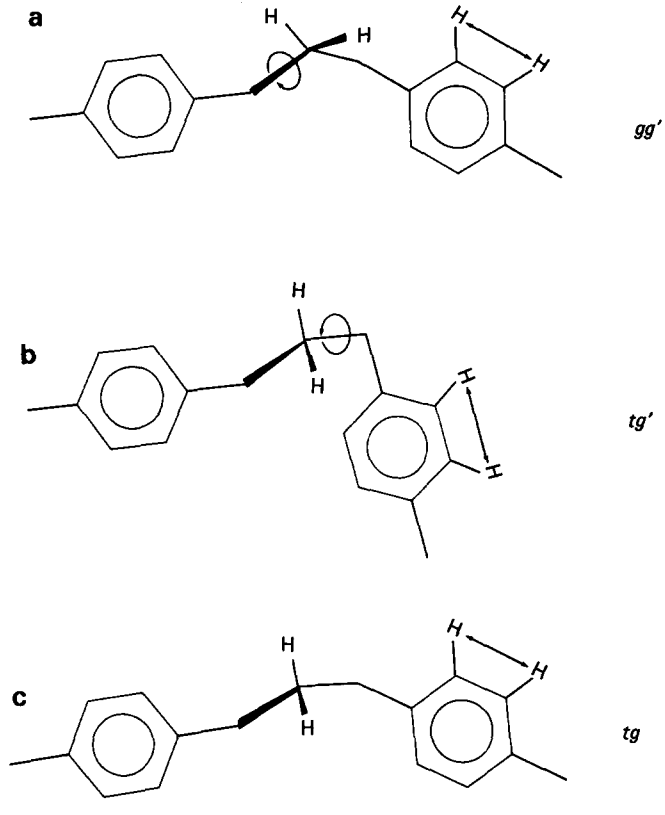

Figure 3 Likely conformational transitions in the formal group. The motional process associated with equation (17) is shown (see text). The arrows indicate the rotations of the conformational changes from (1) to (3). The overall conformational process is *gg'* to *tg* with the intermediate state of *tg'* shown only to indicate the two conformational changes involved in the overall process. The intermediate state, *tg'*, is an unlikely transition state since it involves a large rotation of chain end and some other pathway avoiding the *tg'* intermediate is likely. Nevertheless, the conformation of two bonds change which is the point made by the inclusion of the *tg'* state. Note the proton–proton dipole of the phenylene group is only translated and not reoriented. This is a Helfand Type II motion thought to be a generally plausible form of segmental motion. The overall effect of this motion is two site exchange (*gg'* to *tg*) which is a very restricted rotation far short of isotropic motion

Table 4 Simulation results for PBA–PF as a function of concentration above T_g (130°C)

Wt%	τ_1 (ns)	τ_0 (ns)	τ_{irm} (ns)	τ_{irf} (ns)	τ_{irp} (ns)		
5	0.068	0.30	0.014	0.050	0.039		
10	0.080	0.31	0.022	0.050	0.045		
30	0.125	0.75	0.023	0.075	0.078		
						Angular amplitude	Diffusion constant[a]
50	0.150	2.00	0.026	0.180	175	650	
70	0.360	4.00	0.027	0.330	160	130	
100	0.650	7.50	0.026	1.150	105	40	

[a] In units of 10^8 s^{-1}

where ω_A is the circulation vibration frequency corresponding to the curvature of the potential in the initial state and ω_C is the frequency corresponding to the curvature of the top of the barrier. U_0 is the barrier height and β is the friction constant per unit mass.

If the general Kramers form is utilized, one can rewrite equation (13) for other potentials as

$$\tau = (\eta/K)\exp(U_0/kT) \tag{14}$$

where η is the viscosity experienced by the local motion, K is a constant for a given motion and τ is the correlation time determined by n.m.r.

The viscosity, η, can be written in terms of the Doolittle equation[23],

$$\eta = A\exp[B(V - V_f)/V_f] \tag{15}$$

where V is the total volume, V_f is the free volume and A and B are constants. Combining equations (14) and (15), we obtain for a single given temperature:

$$\tau = A'\exp[B(1-f)/f]$$
$$f = f_1 - c\phi_2 \tag{16}$$

where f is the fractional free volume, f_1 is the fractional free volume of solvent and ϕ_2 is the weight fraction of polymer. A' and c are constants at a given temperature, and A' has a temperature dependence according to equation (14).

Assuming B and f_1 are the same for segmental and formal group motion (both backbone motions), τ_1, τ_0 and τ_{irf} at the various concentrations listed in *Table 4* are fit to equation (16) using a non-linear least square program. *Figure 4* illustrates the results of this procedure.

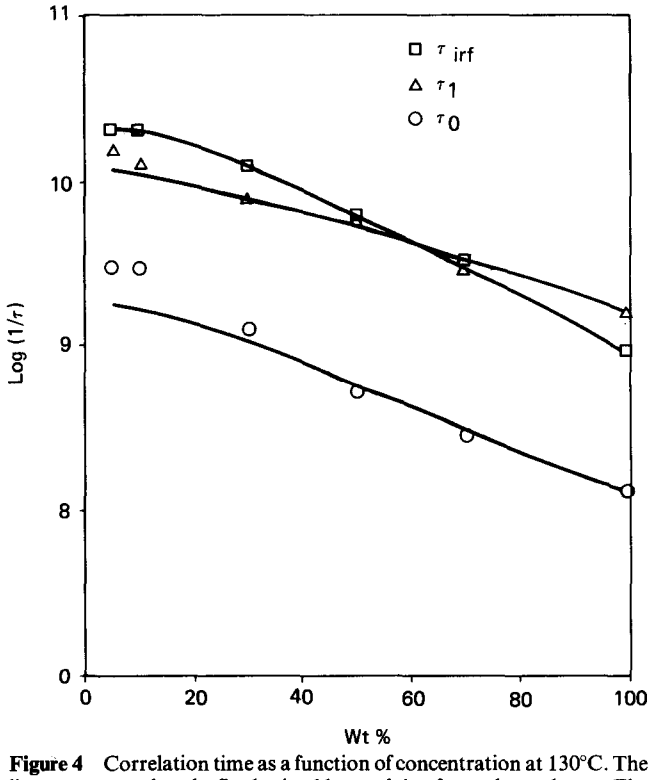

Figure 4 Correlation time as a function of concentration at 130°C. The lines correspond to the fit obtained by applying free volume theory. The points are correlation times for segmental motion (τ_1 and τ_0) and formal group rotation (τ_{irf})

Table 5 Comparison of local motions of polyformals relative to BPA-PC[a]

Polymer	Segmental τ_1/τ_1(BPA–PC)	Phenylene τ_{irp}/τ_{irp}(BPA/PC)	Methyl τ_{irm}/τ_{irm}(BPA–PC)
BPA–PC	1.0	1.0	1.0
BPA–PF	1.62±0.26	1.00±0.10	0.90±0.10
Chloral–PF	1.88±0.42	2.87±0.39	

[a] The ratio is obtained from dividing correlation time for each local motion of BPA–PC (ref. 4) by that in polyformals (this study and ref. 8) at each temperature. Then, the average value and standard deviation in this table are obtained from those ratios in the entire temperature range

Table 6 Comparison of single bond transitions for two polyformals

	BPA–PF	Chloral–PF
T_g	90°C	108°C
Temperature (°C)	τ_0 (ns)	τ_0 (ns)
−20	7.9	25.0
0	5.0	11.0
20	2.78	6.5
40	1.71	4.14
60	1.15	2.77
80	0.79	1.94
100	0.57	1.41
120	0.48	1.06
E_a (kJ mol^{-1})	18.1	17.4
$\tau_\infty \times 10^{14}$ (s)	163	516
Correlation coefficient	0.99	0.99

DISCUSSION

Segmental motion, phenylene, methyl and formal group rotations in BPA–PF can be compared to the local motions in BPA–PC and Chloral–PF. Beginning with the description of segmental motion, several general aspects can be noted. This description involves only bonds in the bisphenol unit so segmental motion should be fairly similar for BPA–PC and BPA–PF. The correlation time for the cooperative transitions, τ_1, is the dominant factor in the simulation of segmental motion while that for the single transitions, τ_0, becomes a relatively minor factor. This may be due to the complexity of repeat unit in the polycarbonates and polyformals relative to polyethylene[30]. The time scale for cooperative transitions in BPA–PF is slower by a factor 1.5–2 relative to BPA–PC throughout the entire temperature range. The time scale in BPA–PF is slightly faster than in Chloral–PF, as is BPA–PC relative to Chloral–PC. *Table 5* shows the ratio of average correlation time and standard deviation relative to BPA–PC for each local motion throughout entire temperature range. The activation energy for cooperative transitions in order from the smallest to the largest value is, BPA–PC, BPA–PF and Chloral–PF. Interestingly, the activation energy for single transitions are nearly identical for these three polymers though the prefactor indicates the time scale for single transitions in BPA–PF is smaller than in Chloral–PF. Since the glass transition is correlated with single bond transitions in the structural analogues of polycarbonate[5,6], the lower T_g would correspond to faster single bond transitions. This agrees well with the lower T_g in BPA–PF (90°C) compared to T_g in Chloral–PF (108°C). *Table 6* illustrates the time scale of single bond transitions for both polyformals.

Table 7 Comparisons of simulation parameters of polycarbonate and polyformals

Segmental motion						
		Apparent activation energy (kJ mol^{-1})		Arrhenius prefactor ($\tau^*_\infty \times 10^{14}$ s)		
Polymer	T_g (°C)	Cooperative segmental (τ_1)	Single backbone rotation (τ_0)	Cooperative segmental (τ_1)	Single backbone rotation (τ_0)	Ref.
BPA–PC	150	19	16	28	1003	4
BPA–PF	90	23	18	8	163	
Chloral–PF	108	25	17	5	516	8

Phenylene group motion					
	T_γ[a] (°C)	Type	E_a (kJ mol^{-1})	$\tau^*_\infty \times 10^{14}$	Ref.
BPA–PC	−100	Stochastic diffusion	22	6	4
BPA–PF	−100	Stochastic diffusion	21	6.6	
Chloral–PF	−100	Stochastic diffusion	21	19	8

[a] Temperature of the main sub-glass transition loss peak measured at 1 Hz (ref. 26)

There is an activation energy difference between τ_1 and τ_0. This is somewhat different from polycarbonates where the activation energies are found to be nearly equal. In the polycarbonates, the similarity of τ_1 and τ_0 in activation energy is indicative of sequential cooperative motions as opposed to simultaneous[27–29]. This activation energy difference is also found in the solution study of another structure analogue, Chloral–PF[8]. For both polyformals, the activation energy for cooperative transitions is higher than for the single transitions which may be indicative of more nearly simultaneously cooperative transitions such as crankshaft motions. *Table 7* displays these comparisons.

For methyl group rotation, the time scale and activation energy are nearly the same between BPA–PF and BPA–PC. This indicates that the methyl group rotation is a localized process and is essentially unaffected by changing from a carbonate link to a formal link.

At low concentrations, the phenylene group rotation is best modelled by stochastic diffusion. As in the previous study on Chloral–PF[8], the phenylene T_1's are best simulated without a contribution from formal group motion. The activation energy is nearly identical with polycarbonates and Chloral–PF. This is not surprising since the phenylene group rotation has been suggested to be a very localized process[4,8]. The time scale of phenylene group rotation in BPA–PF is almost identical to BPA–PC. On the other hand, the time scale of phenylene group rotation in Chloral–PF is a little slower but within a factor of 3 relative to BPA–PC. *Table 5* lists these comparisons.

The activation energy for formal group rotation in BPA–PF is 3 kJ mol^{-1} lower than in Chloral–PF leading to a faster time scale for formal group rotation in BPA–PF though within a factor of 3 of that in Chloral–PF. It is clear that the formal group motion is faster in BPA–PF than in Chloral–PF. However, since both polyformals have similar conformational energy surfaces, the possible conformational changes for the formal group in Chloral–PF can be proposed to be the same as in BPA–PF[8]. The most plausible conformational changes in both polyformals are represented by

$$gg' = tg' = tg \quad (17)$$

$$gg' = gt = g't \quad (18)$$

Figure 3 illustrates local formal group motion in a repeat unit resulting from conformational state changes in equation (17). The lowest conformational state is gg' as shown in *Figure 3a* according to a conformational energy map of a related small molecule, dimethyoxymethane[40]. The gg' state undergoes *trans–gauche* rotation to form tg' in *Figure 3b*. The second rotation about the neighbouring C–O bond changes tg' to tg. This second rotation does not reorient the dipole in the formal group. Note that the initial state is gg' and the final state is tg. The intermediate state shown, tg', is not a realistic intermediate since it would involve a large rotation of the chain end. Rather the tg' is given here to set up the geometry of the correlation function and represents a suitable mathematical pathway from gg' to tg. In the overall formal group motion, the proton–proton dipole of the phenylene group is translated but not reoriented in the overall conformational change and will not cause phenylene group relaxation which is consistent with our interpretation of phenylene group motion. This proposed formal group motion is a Type II motion in the Helfand nomenclature[27] and Type II motions are very important in the computer simulation of segmental motion in polyethylene chains. Another similar process can occur when gg' undergoes two 120° bond rotations to form $g't$ as shown in equation (18). If one combines the processes in equations (17) and (18), there are two possible isomerization mechanisms to cause the formal group reorientation. This physical picture is consistent with the mathematical interpretation of double *trans–gauche* rotations on the formal group developed with the Szabo formalism. This is a very localized restricted anisotropic motion and therefore it has been treated separately from isotropic segmental even though both involve backbone bonds.

The geometry of phenylene group motion related to the conformational changes is further investigated by utilizing matrix transformations of the dipolar vector[41]. The phenylene ring is rotated 64° out of its original plane by the conformational process. If the phenylene group is not reoriented by formal group rotation as in the Chloral–PF and present studies, we would expect some certain degrees of phenylene ring rotation about the C_1C_4 axis along with formal group rotation. This picture indicates coupling between formal group and phenylene

group motion, and the time scale of both motions determined from the n.m.r. data is within a factor of two throughout the entire temperature and concentration range. The displacement of phenylene ring after conformational changes is 2.18 Å which is reasonable for the translation of a chain end.

The *trans–gauche* isomerization of the formal group in polyformal is somewhat different from the proposed *trans–cis* isomerization of carbonyl group in the polycarbonate[42]. On the other hand, the polyformals have a similar dynamic mechanical spectrum to the polycarbonates[26]. In view of this similarity, the local motions of polyformals should not be very different from those in the polycarbonates. Additional spin-relaxation and line shape studies of glassy polyformal might be able to shed additional light on the differences and similarities of these two polymers.

In the concentration study, segmental motion, methyl group rotation and formal group rotation can be simulated within experimental error by using the same approach as in dilute solution. The phenylene group data can only be simulated in the samples below 30 wt% by using stochastic diffusion. In the higher concentration samples, large deviations in simulation appear if the stochastic diffusion model is employed. Several approaches were considered to reduce the deviations. First, it might suggest that there is a distribution of correlation times due to the difference in the local environment. Hence, we adopted the correlation function developed by Ngai for condensed matter[31,32].

$$\phi(t)=\phi(0)\exp(-t/\tau_p)^{\alpha}$$

This correlation function has been successfully applied in the glassy state of polycarbonates[33,34] with α controlling the breadth of distribution times and τ_p as the central correlation time. The fractional exponential function was applied in the stochastic diffusion description for phenylene group motion by setting $\tau_p=\tau_{irp}$. Although this approach improves the simulation, it still leaves about a 20% deviation from experimental T_1.

Yaris had developed a damped diffusion model for polymer backbone motion[37–39] which tries to include intermolecular effects and may therefore improve the fit of the concentration dependent data. To apply this model, the Hall–Helfand correlation function was replaced by the normalized orientation autocorrelation function derived from damped diffusion and complex damped diffusion models. The stochastic diffusion model for the phenylene group rotation was retained and the data in *Table 2* resimulated. We find that both damped diffusion and complex damped diffusion models give very similar fits though still leave large deviations in the high concentration of phenylene T_1 data. This similarity between the Hall–Helfand model and the Yaris–Skolnick model had been pointed out in a mathematical comparison of the functions[43]. The parameter γ in the Yaris–Skolnick model decreases with increasing concentration as noted in an analysis of relaxation in dissolved poly(vinyl acetate) but the physical significance of γ is difficult to identify.

The surroundings of the polymer chain change drastically as concentration is raised yet the dilute solution approach largely appears to carry over to the bulk. The main difference in the character of motion as concentration is raised arises from the phenylene group. In the dilute solution, the potential for stochastic diffusion is the same for each orientation of phenylene ring about the C_1C_4 axis. In high concentration the potential may not be the same due to interchain interactions. Two fold jump between the minima, 0° and 180°, was applied but the simulation results were not reasonable[35]. Another model considered was the restricted rotation in a square well potential, developed by Gronski[20]. This model combined with Hall–Helfand segmental description can simulate phenylene T_1 in the higher concentration within experimental error. The restricted rotation model has been used in other solution studies of structural analogues of polycarbonate including substitutents on the phenylene ring[5], and a bulky group between the two phenylene rings[6]. In the polyformal at high concentrations it would appear that phenylene ring rotation is reduced to phenylene ring libration resulting from intermolecular interactions. Ring rotation may continue at high concentrations but at a rate too slow to contribute to T_1 while ring libration continues at a sufficiently rapid rate.

With the Hall–Helfand segmental description and a change in phenylene group motion from complete to restricted anisotropic motion, several other comments can be made on the concentration dependence of the local motions. The time scales for cooperative transitions and single bond transitions are still fast (nanoseconds) throughout the entire concentration range and only decrease by about one order of magnitude. This time scale is normal since the concentration dependence of the relaxation time may be quite small for the highly mobile chain above the glass transition temperature[25]. The applicability of the same general description of segmental motion is interesting but, as the glass transition is approached the nature of segmental motion must change drastically. The changes must involve both time scale and spatial restriction and would be an important subject for further investigation.

Other local motions such as formal group and phenylene group rotations also decrease as the polymer concentration increases. The time scale of formal group rotation decreases by about one order of magnitude. The angular amplitude of phenylene rotation is reduced from 175° at 50 wt% to 105° at 100 wt%. The diffusion constant also changes significantly from $6.5\times10^{10}\,s^{-1}$ at 50 wt% to $4.0\times10^{8}\,s^{-1}$ at 100 wt%. These diffusion constant values are reasonable for the phenylene ring motion at that concentration and temperature[33,34].

Another interesting point is the negligible change of methyl group rotation throughout the entire concentration range. In the solution study of polycarbonates[4], it was found that the methyl group rotation might not be affected by concentration although the highest concentration was considered only 30 wt%. In this study, we found the time scale of methyl group rotation changes from 0.020 ns at 5 wt% to 0.026 ns at 100 wt%, indicating independence of this motion from segmental motion and from the surrounding medium. A qualitative comment on the effect of concentration changes can be made. Segmental motion likely involves one to several repeat units and will sweep out a significant volume as it occurs. Methyl group rotation involves only a part of the repeat unit and sweeps out little volume as it occurs. Phenylene and formal group rotations apparently sweep more volume than methyl group rotation and would also be affected by the medium. From this

standpoint, the apparent concentration dependence is reasonable though the concepts utilized in the comment are not quantitative.

Free volume theory has been applied in dielectric relaxation[24,25], viscoelastic relaxation[37], and n.m.r. relaxation[13] studies but not to a system with as detailed a description of complex local motion as BPA–PF. In order to apply free volume theory, the correlation times for three types of backbone motions were considered (τ_1, τ_0 and τ_{iff}). The constant B and fractional free volume of solvent f in free volume theory are assumed to be the same for the three backbone motions. This assumption is reasonable since both parameters should be the same as long as local motions are segmental rearrangements. *Figure 4* shows the fitting of three local motions using equation (16) which yield $f_1 = 0.38$ for the fractional free volume of solvent and an average value of $f_2 = 0.28 \pm 0.01$ for the fractional free volume of pure polymer. The value of f_1 is quite reasonable compared to other systems in comparable solvents[13,26]. The value of f_2 is a little higher though the measurements were performed at a high temperature and it is difficult to compare with other systems.

A free volume description of phenylene group rotation is not possible since the motion contributing to spin-relaxation changes from complete anisotropic rotation to restricted anisotropic rotation.

The above discussion suggests that a free volume approach can describe the correlation times for local motion above the glass transition developed from multifield spin-lattice relaxation data. It is important to note that free volume theory applies to the correlation times and not to the T_1 data directly. For BPA–PF, the dependence of free volume on composition and temperature is not established from other techniques so independent comparisons have not been made. It would be interesting to see if free volume parameters from thermodynamic or long range relaxation data matched those determined from local motions in this system.

ACKNOWLEDGEMENTS

This research was carried out by the financial support of National Science Foundation Grant No. DMR-790677, of National Science Foundation Equipment Grant No. CHE-77-09059 and of National Science Foundation Grant No. DMR-8108679. We thank the Worcester Consortium for use of SXP 20-100 and WM-250 spectrometers, and Mr Frank Shea for his help. We also thank Yale University for use of WM-500 spectrometer, and Mr Peter Demou for his assistance.

REFERENCES

1 Heatley, F. *Prog. NMR Spectrosc.* 1979, **13**, 47
2 Jones, A. A. and Bisceglia, M. *Macromolecules* 1979, **12**, 1136
3 O'Gara, J. F., Dejardins, S. G. and Jones, A. A. *Macromolecules* 1981, **14**, 64
4 Connolly, J. J., Gordon, E. and Jones, A. A. *Macromolecules* 1984, **17**, 722
5 Roy, A. K. and Jones, A. A. *J. Polym. Sci., Polym. Phys. Edn.* 1985, **23**, 1793
6 Connolly, J. J. and Jones, A. A. *Macromolecules* 1985, **18**, 906
7 Tarpey, M. F., Lin, Y.-Y., Jones, A. A. and Inglefield, P. T., 'NMR and Macromolecules', (Ed. J. C. Randall), American Chemical Society: Washington, DC (1984), ACS Symp. Ser. No. 247, p. 67
8 Hung, C.-C., Shibata, J. H., Tarpey, M. F., Jones, A. A., Porco, J. A. and Inglefield, P. T., submitted to *Anal. Chim. Acta*
9 Komoroski, R. A. and Mandelkern, L. *J. Polym. Sci., Polym. Symp. Edn.* 1976, **54**, 227
10 Jones, A. A., Lubianez, R. P., Hanson, M. A. and Shostak, S. L. *J. Polym. Sci., Polym. Phys. Edn.* 1978, **16**, 1685
11 Jones, A. A., Robinson, G. L. and Gerr, F. E. *Am. Chem. Soc. Sym. Ser.* 1979, **103**, 271
12 Heatley, F. *Polymer* 1975, **16**, 493
13 Blum, F. D., Darairaj, B. and Padmanabhan, A. S. *Macromolecules* 1984, **17**, 2837
14 Schafer, J. *Macromolecules* 1973, **6**, 882
15 Anderson, J. E., Liu, K.-J. and Ullman, R. *Disc. Faraday Soc.* 1970, **49**, 257
16 Hall, C. K. and Helfand, E. *J. Chem. Phys.* 1982, **77**, 3275
17 Weber, T. A. and Helfand, E. *J. Phys. Chem.* 1983, **87**, 2881
18 Woessner, D. E. *J. Chem. Phys.* 1962, **36**, 1
19 Szabo, A. *J. Chem. Phys.* 1984, **81**, 1
20 Gronski, W. and Murayama, N. *Makromol. Chem.* 1978, **179**, 1521; Gronski, W. *Makromol. Chem.* 1979, **180**, 1119
21 Kramers, M. A. *Physica* 1940, **7**, 284
22 Kramers, M. A. *Physica* 1956, **22**, 29
23 Doolittle, A. K. and Doolittle, D. B. *J. Appl. Phys.* 1957, **28**, 901
24 Stockmayer, W. H. *Pure Appl. Chem. Macromol. Chem.* 1973, 379
25 Stockmayer, W. H. *Pure Appl. Chem.* 1967, **15**, 539
26 Yee, A. F. and Smith, S. A. *Macromolecules* 1981, **14**, 54
27 Helfand, E. *J. Chem. Phys.* 1971, **54**, 4651
28 Helfand, E., Wasserman, Z. R. and Weber, T. A. *Macromolecules* 1980, **13**, 526
29 Skolnik, J. and Helfand, E. *J. Chem. Phys.* 1980, **72**, 5489
30 Lin, Y.-Y., Jones, A. A. and Stockmayer, W. *J. Polym. Sci., Polym. Phys. Edn.* 1984, **22**, 2195
31 Ngai, K. L. *Comm. Solid State Phys.* 1979, **9**, 127
32 Ngai, K. L. *Phys. Rev. B.* 1980, **22**, 2066
33 Jones, A. A., O'Gara, J. F., Inglefield, P. T., Bendler, J. T., Yee, A. F. and Ngai, K. L. *Macromolecules* 1983, **16**, 685
34 O'Gara, J. F., Jones, A. A., Hung, C.-C. and Inglefield, P. T. *Macromolecules* 1985, **18**, 1117
35 Jones, A. A. *J. Polym. Sci., Polym. Phys. Edn.* 1977, **15**, 863
36 Ferry, J. D., 'Viscoelastic Properties of Polymers', Ch. 11 and 17, Wiley, New York (1980)
37 Skolnick, J. and Yaris, R. *Macromolecules* 1982, **15**, 1041; *erratum* 1983 **16**, 491
38 Skolnick, J. and Yaris, R. *Macromolecules* 1982, **15**, 1046; *erratum* 1983, **16**, 492
39 Skolnick, J. and Yaris, R. *Macromolecules* 1983, **16**, 266
40 Tvarosk, I. and Bleha, T. J. *J. Molec. Struct.* 1975, **24**, 249
41 Flory, P. J., 'Statistical Mechanics of Chain Molecules', Wiley, New York, 1969, Ch. 1, p. 19
42 Jones, A. A. *Macromolecules* 1985, **18**, 902
43 Skolnick, J. and Yaris, R. *Macromolecules* 1985, **18**, 1635